NANO LETTERS

2008
Vol. 8, No. 8
2473-2478

Assembly of Polypeptide-Functionalized Gold Nanoparticles through a Heteroassociation- and Folding-Dependent Bridging

Daniel Aili,[†] Karin Enander,[†] Lars Baltzer,[‡] and Bo Liedberg*[,†]

Division of Sensor Science and Molecular Physics, Department of Physics, Chemistry and Biology, Linköping University, SE-581 83 Linköping, Sweden, and Division of Organic Chemistry, Department of Biochemistry and Organic Chemistry, BMC, Box 576, Uppsala University, SE-751 23 Uppsala, Sweden

Received May 23, 2008

ABSTRACT

Gold nanoparticles were functionalized with a synthetic polypeptide, de novo-designed to associate with a charge complementary linker polypeptide in a folding-dependent manner. A heterotrimeric complex that folds into two disulphide-linked four-helix bundles is formed when the linker polypeptide associates with two of the immobilized peptides. The heterotrimer forms in between separate particles and induces a rapid and extensive aggregation with a well-defined interparticle spacing. The aggregated particles are redispersed when the disulphide bridge in the linker polypeptide is reduced.

Self-assembly has evolved into an interesting alternative for nanofabrication, and has in recent years been employed extensively for the construction of complex hybrid materials and nanocomposites.[1,2] Gold nanoparticles have been utilized as a component in many such materials because of their attractive physical and chemical properties that are of interest for novel optical and sensing applications.[3,4] In addition, the surface chemistry of gold nanoparticles can be tailored with great precision,[5] which has allowed their functionalization with a wide variety of biomolecules including DNA,[6,7] proteins,[8] peptides,[9–11] and carbohydrates,[12,13] for the development of functional materials[14–16] and for studies of macromolecular interactions at interfaces.[8,17] Because highly complex nanostructures can be found in nature, it is not surprising that much of the work on nanosized self-assembling systems has been based on biological or biomimetic building blocks and biomolecular interactions. Proteins are by far the most complex and versatile group of biomolecules when considering their structural properties and chemical and biological functionalities. A drawback of many proteins is, however, their lack of structural robustness. Most proteins are very sensitive to changes in their physiochemical environment and can easily and irreversibly lose their native conformation. In this perspective, designed polypeptides that adopt an ordered secondary and tertiary structure have emerged as an interesting alternative. Synthetic polypeptides have the same chemical flexibility as proteins but are typically more robust. As the design rules for obtaining functional and folded polypeptides gradually are being elucidated, novel polypeptides with new shapes and functions have been constructed[18] and have in recent years been exploited for the development of self-assembling nanostructures[19] and hybrid materials.[9,10]

In this paper, we report on the reversible assembly of polypeptide-decorated gold nanoparticles using a polypeptide linker that associates with the immobilized peptides in a folding-dependent manner. The polypeptides are de novo-designed to form a heterotrimeric complex consisting of two identical helix−loop−helix polypeptides that are connected through one charge-complementary linker polypeptide. Upon hetero-association, folding into two disulphide-linked four-helix bundles occurs as described schematically in Figure 1a. The bridging of particles through the formation of the heterotrimer is demonstrated as an effective route for controlling nanoparticle assembly under physiological conditions that affords both specificity and reversibility.

We have previously described how folding, as a result of homodimerization between immobilized polypeptides, can induce a reversible assembly of nanoparticles.[20] The present finding, that a folding-dependent heteroassociation can be utilized as the driving force for nanoparticle assembly, adds

* Corresponding author. E-mail: bol@ifm.liu.se.
[†] Linköping University.
[‡] Uppsala University.

10.1021/nl8014796 CCC: $40.75
Published on Web 06/26/2008

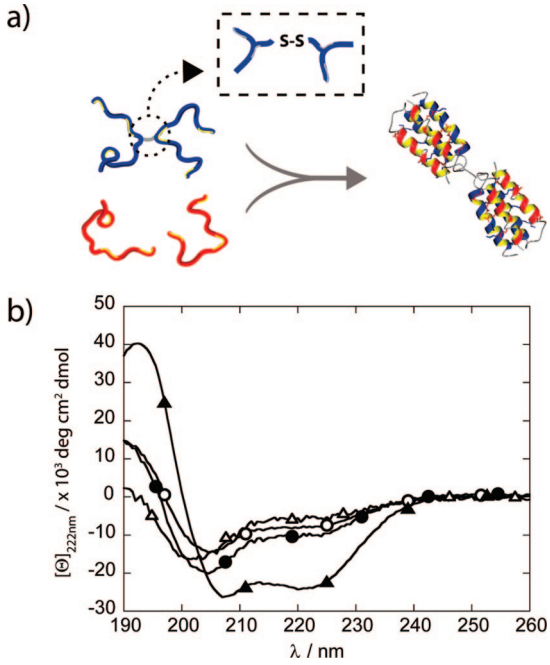

Figure 1. (a) The linker polypeptide associates with two helix−loop−helix polypeptides, and the complex folds into a heterotrimer consisting of two disulphide-linked four-helix bundles. (b) CD spectra of (Δ) JR2EC (100 μM), (▲) JR2EC (100 μM) + $JR2KC_2$ (50 μM), (●) $JR2KC_2$ (50 μM), and (○) JR2ECref (100 μM) + $JR2KC_2$ (50 μM).

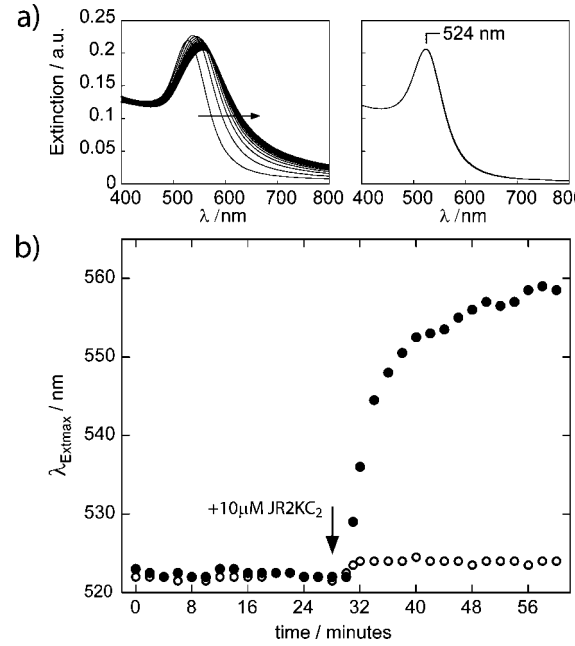

Figure 2. (a) JR2EC-decorated particles (left) and JR2ECref-decorated particles (right), in HBS-EP after addition of 10 μM $JR2KC_2$. Spectra were recorded every 2 min for 30 min. (b) The change in position of the extinction maximum illustrates the kinetics of aggregation for particles functionalized with (●) JR2EC and (○) JR2ECref in HBS-EP before and after addition of 10 μM $JR2KC_2$.

an additional piece to this nanocomposite Lego. The chemical and structural flexibility of the designed polypeptides, and the possibility to utilize polypeptide folding to control nanoparticle assembly, are valuable new tools for nanoengineering and the development of new materials.

JR2EC is a de novo-designed glutamic-acid-rich 42-residue helix−loop−helix polypeptide with a net charge of −5 at neutral pH. JR2EC is a random coil at pH 7 but can homodimerize and fold into a molten globule-like four-helix bundle at slightly acidic pH (<6) or at neutral pH in the presence of Zn^{2+}.[20,21] JR2EC is also designed to heterodimerize at neutral pH with the charge-complementary, lysine-rich polypeptide JR2KC.[22,23] At neutral pH, JRKC has a net charge of +11 and is a random coil, but heterodimerization induces folding of the peptides into a molten globule-like four-helix bundle.[23–25] The driving force for folding is mainly the formation of a hydrophobic core constituted by the hydrophobic inner sides of the amphiphilic helices, but the formation of salt bridges is also important. The dissociation constant (K_d) for heterodimerization in solution is 0.02 mM.[22] A key residue in JR2EC and JR2KC is a cysteine in position 22, located in the loop region. This residue enabled site-specific, thiol-dependent immobilization of JR2EC on gold nanoparticles and was furthermore utilized to create the linker polypeptide $JR2KC_2$ by covalently joining two identical monomers through a disulphide bond (Figure 1a). Oxidation of the cysteines into a disulphide was performed by dissolving the lyophilized peptide in 0.1 M ammonium bicarbonate buffer pH 8, followed by aeration for 90 min. The peptides were then incubated for 72 h. Complete oxidation was confirmed by a conventional Ellman's test.[26]

To investigate the impact of folding on particle assembly, an additional polypeptide with the same primary sequence as JR2EC, but without folding ability, was utilized. In this peptide, designated JR2ECref, all L-alanine residues were exchanged by D-alanine, while keeping all other amino acids in the L-state. By mixing D- and L-amino acids in the sequence the polypeptide is prevented from folding into four-helix bundles under any circumstances.[20,21] All peptides were synthesized on the solid phase and cleaved from the resin by 95% trifluoroacetic acid, purified by reversed-phase HPLC, and identified from their matrix-assisted laser desorption/ionization time-of-flight (MALDI-TOF) spectra. Amino acid sequences and details on synthesis are presented in the Supporting Information.

On planar gold surfaces, JR2EC and JR2ECref form submonolayers with similar properties regarding coverage and organization.[20] The ability of JR2EC to fold into either a hetero- or homodimer is retained when immobilized on gold substrates.[22] When immobilized on gold nanoparticles, aggregation can be utilized to induce folding of JR2EC as a result of dimerization between peptides immobilized on adjacent particles.[21] Furthermore, at neutral pH and in the presence of Zn^{2+}, homodimerization and folding of immobilized JR2EC has been demonstrated as a means to induce a reversible nanoparticle aggregation.[20]

In solution at neutral pH, and when kept separately, JR2EC and $JR2KC_2$ displayed random-coil CD spectra, typical for unordered polypeptides (Figure 1b). When mixing JR2EC and $JR2KC_2$ at a 2:1 ratio, the polypeptides adopted an α-helical spectrum with a mean residue ellipticity at 222 nm ($[\Theta]_{222nm}$) of approximately −24 000 ± 1000 °·cm^2·dmol^{-1}.

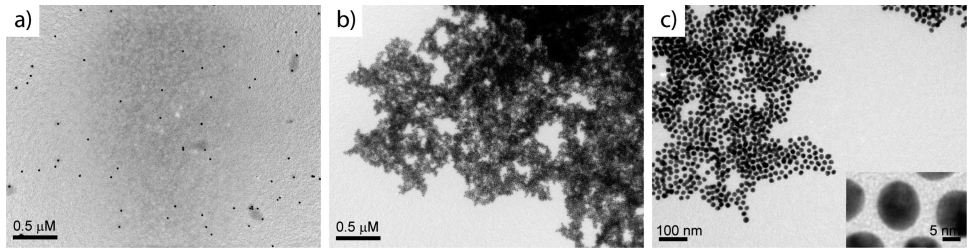

Figure 3. Electron micrographs of particles functionalized with (a) JR2ECref, (b and c) JR2EC, after incubation with $JR2KC_2$ for 20 min and dried on carbon-coated TEM grids. No aggregates were obtained using the reference polypeptide JR2ECref, whereas massive aggregates were observed for the JR2EC functionalized particles. Inset: The average interparticle distance is 4.6 ± 0.2 nm.

No ordered secondary structure was observed when replacing JR2EC by the reference peptide JR2ECref, strongly suggesting that no specific interactions take place between $JR2KC_2$ and JR2ECref.

Gold nanoparticles display a strong extinction in the visible spectrum due to collective electron oscillations, or localized surface plasmon resonance (LSPR), as described by Mie theory.[27] The resonance wavelength and bandwidth are dependent on the particle size and shape, the refractive index of the surrounding medium, and the temperature.[4,28] Particle aggregation typically results in a massive redshift of the LSPR peak position as well as a peak broadening, caused by the near-field coupling between adjacent particles. The magnitude of the redshift is highly dependent on the interparticle distance and the size of the aggregates. The smaller the distance and the bigger the aggregates, the larger the resulting redshift.[29–31]

JR2EC and JR2ECref were immobilized by incubating the as-prepared particles (~13 nm in diameter) in a 100 μM peptide solution in 10 mM citrate buffer at pH 6 overnight. To remove excess peptides, we centrifuged the particles repeatedly and replaced the supernatant with fresh 30 mM bis−tris buffer pH 7, until the concentration of unbound peptides was negligible (<0.5 nM). The peptide-modified particles were highly stable and could withstand both repeated centrifugations and long storage (several months) without showing any detectable aggregation. After functionalization, the plasmon peak was slightly red-shifted from 519−520 nm to around 523−524 nm, which is probably due to both the change in refractive index upon binding of the peptides and change of buffer. Minor changes in the particle size distribution as a result of the repeated centrifugations may also contribute.[32]

When both JR2EC and JR2KC are oxidized, the polypeptides assemble into micrometer-long fibers upon mixing as a result of a propagating folding-mediated heteroassociation;[33] whereas if only JR2KC is oxidized, no fibers can be formed but rather two disulphide-linked four-helix bundles composed of two JR2EC molecules linked by $JR2KC_2$. Because $JR2KC_2$ can bind two molecules of JR2EC, it was utilized in order to investigate the possibility to assemble gold nanoparticles modified with JR2EC through a specific and folding-mediated bridging. The polypeptide-decorated gold nanoparticles were dispersed in HBS-EP (10 mM Hepes, 0.15 M NaCl, 3 mM EDTA, and 0.005% surfactant P20, pH 7.4. GE-Healthcare), which resulted in a slight blueshift of the LSPR peak to approximately 522 nm. No decrease in particle stability was observed due to the buffer, despite physiological concentrations of NaCl. Extensive aggregation was, however, induced upon addition of $JR2KC_2$, which resulted in a major redshift of the LSPR peak to approximately 560 nm within a couple of minutes (Figure 2a, left). In contrast, no aggregation of particles modified with the reference peptide (JR2ECref) was observed. The slight redshift of the plasmon peak to approximately 524 nm (Figure 2a, right) is attributed to nonspecific association of $JR2KC_2$ to the reference peptide in combination with the change in refractive index of the buffer upon addition of the peptides. The differences in both rate and extent of aggregation are illustrated clearly in Figure 2b, showing the change in wavelength of maximum extinction (λ_{Extmax}) as a function of time. On the basis of these observations, aggregation as a result of an unspecific (e.g., electrostatic) bridging by $JR2KC_2$ can be ruled out. The ability of the peptides to fold correctly is obviously necessary because aggregation was induced only for particles functionalized with JR2EC.

In good agreement with UV−vis data, no aggregates could be observed in transmission electron micrographs (TEM) of the JR2ECref-modified particles (Figure 3a). However, when using JR2EC, the folding-dependent bridging resulted in very large aggregates, containing many thousands of particles that typically displayed a regular interparticle distance (Figure 3b and c). In areas where particles had assembled in a 2D geometry, the average interparticle distance was estimated to be 4.6 ± 0.2 nm, which is in good agreement with the expected distance for particles held together by two disulphide-linked four-helix bundles. For example, the distance between particles separated by a single four-helix bundle was recently found to equal 2.3 ± 0.1 nm,[21] and a monolayer of the heterodimeric four-helix bundle on planar gold substrates had an ellipsometric thickness of 2.3 ± 0.3 nm.[22]

Extensive particle aggregation was induced for concentrations of $JR2KC_2$ in the interval 50 nM to 10 μM, whereas at lower concentrations only small changes in the LSPR peak could be seen (Figure 4a). The surface coverage of monomeric JR2EC on planar gold substrates is approximately 60% of a full monolayer, and the monomer has an estimated footprint of 2 × 2 nm^2.[22] It is reasonable to believe that the coverage on 13-nm gold nanoparticles would not differ very much from this value.[34] Because the concentration of particles was 0.67 nM in all experiments ($\epsilon_{AuNP} = 2.4 \times 10^8$ M^{-1} cm^{-1}),[31] the concentration of JR2EC was thus kept constant

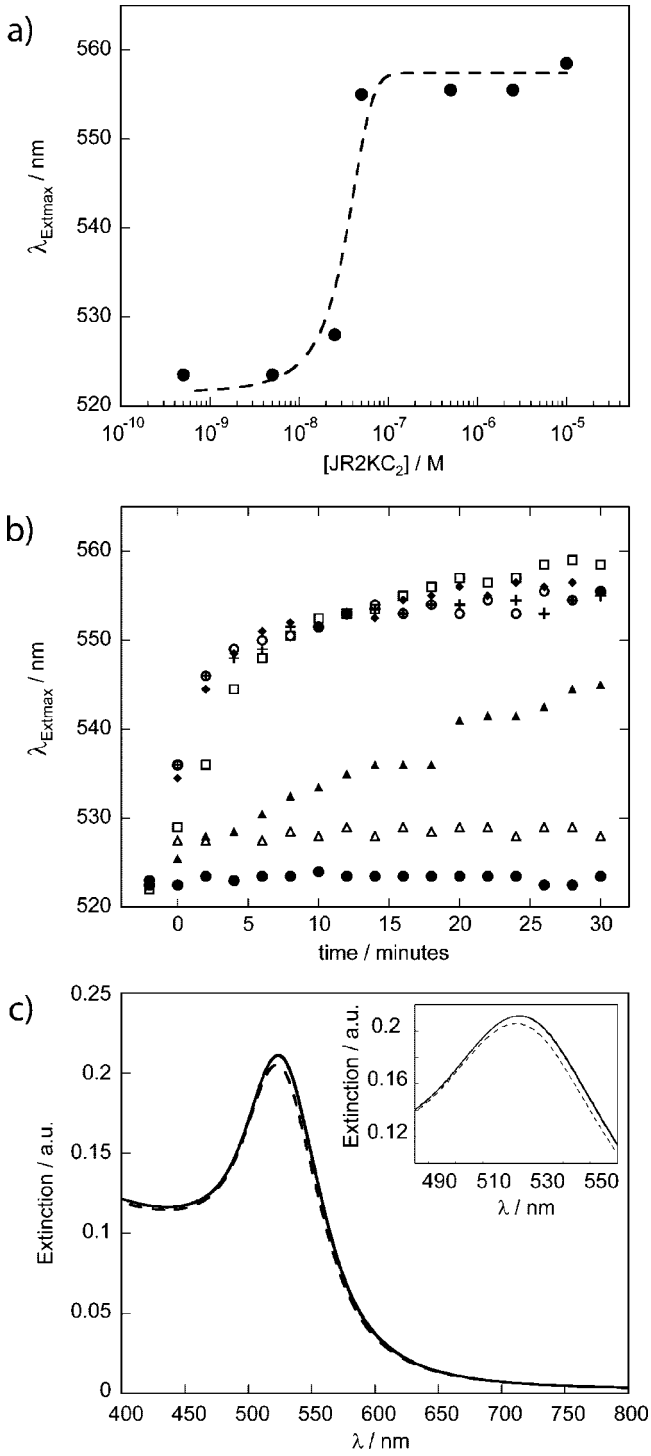

Figure 4. (a) Shift in extinction maximum as a function of the concentration of JR2KC$_2$ (line drawn as guide for the eye). (b) Rate of aggregation for different concentrations of JR2KC$_2$. (▲) 25 μM, (□) 10 μM, (○) 2.5 μM, (♦) 0.5 μM, (+) 50 nM, (Δ) 25 nM, (●) 5 nM. (c) Before (- - -) and after (—) addition of JR2K (2.5 μM). Inset: Closer view on the induced LSPR peak-shift.

at ~0.2 μM. For K_d = 0.02 mM, 75% of all particles will then have at least one JR2KC$_2$ bound at a concentration of JR2KC$_2$ of 50 nM, which evidently is enough to cause an extensive aggregation. The rate of aggregation, as determined from the change in the redshift of the LSPR peak with time, was almost identical for concentrations of JR2KC$_2$ in the interval 50 nM to 10 μM, indicating that the rate-limiting step is not the association of the linker peptide but rather the diffusion of the particles (Figure 4b). This suggests that JR2KC$_2$ first associates with one JR2EC molecule immobilized on one particle, which then associates with a second JR2EC molecule immobilized on the other particle to form the heterotrimeric complex. When more than one linker peptide bridges between the particles, a strong synergistic effect on the total binding strength was obtained. The aggregation could thus not be reversed by the addition of an excess of JR2E or JR2K (polypeptides identical to JR2EC and JR2KC except that the cysteine residue has been replaced by a valine) (data not shown). At a higher concentration of JR2KC$_2$ (25 μM), both the rate and the extent of aggregation were decreased. Because JR2KC$_2$ has a rather high positive net charge, this is most likely due to a charge reversal of the particles from slightly negative to positive when a large amount of the linker peptide is bound. This might improve the electrostatic stabilization of the particles and slow down the rate of aggregation significantly (Figure 4b).

Replacing the disulphide-containing linker peptide JR2KC$_2$ by JR2K resulted in a small redshift in the LSPR peak of ~1−2 nm (Figure 4c). This shift can be explained partly by a buffer effect and partly by the dimerization of JR2K with the immobilized JR2EC. However, no particle aggregation was observed because JR2K can not bridge the particles as JR2KC$_2$. If JR2KC$_2$ would bind to two peptides located on the same particle, then the response would be analogous to the binding of JR2K, which strongly suggests that what drives the nanoparticle assembly is the ability of JR2KC$_2$ to specifically bind to two peptides located on two separate particles as described schematically in Figure 5.

The importance of the disulphide bridge in JR2KC$_2$ was further confirmed by the complete redispersion of the aggregated particles when reducing the linker peptide with tris(2-carboxyethyl)phosphine (TCEP) (Figure 6). The disassembly of the aggregates was, however, very slow (~72 h), further indicating a strong synergistic effect because of the formation of multiple contact points between the particles. A complete reversal of aggregation requires all bridging linker peptides to be reduced. About 20 h after the addition of the reducing agent, the majority of the aggregates were redispersed. A complete reversal of aggregation and a return of the LSPR maximum to ~523 nm was, however, not observed until after approximately 72 h (Figure 6, Inset). A minor decrease in intensity also could be seen, which is most likely due to a small dilution of the particles upon addition of the reducing agent.

In conclusion, a novel supramolecular strategy for the assembly of nanoparticles has been described, exploiting the specific interactions of polypeptide-folding. Gold nanoparticles were functionalized with a de novo-designed polypeptide that forms a heterotrimer with a complementary linker peptide. Upon association, the peptides fold into two disulphide-linked four-helix bundles. The linker peptide associates with the immobilized peptides in a folding-dependent manner and induces aggregation as it bridges between the particles.

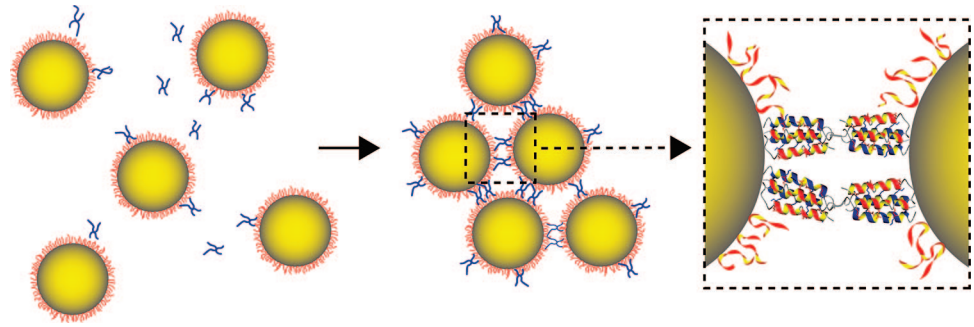

Figure 5. Rapid and folding-dependent particle aggregation was observed upon addition of the linker polypeptide $JR2KC_2$ to nanoparticles functionalized with the complementary polypeptide JR2EC. $JR2KC_2$ associates with two JR2EC polypeptides immobilized on separate nanoparticles, and the complex folds into two disulphide linked four-helix bundles.

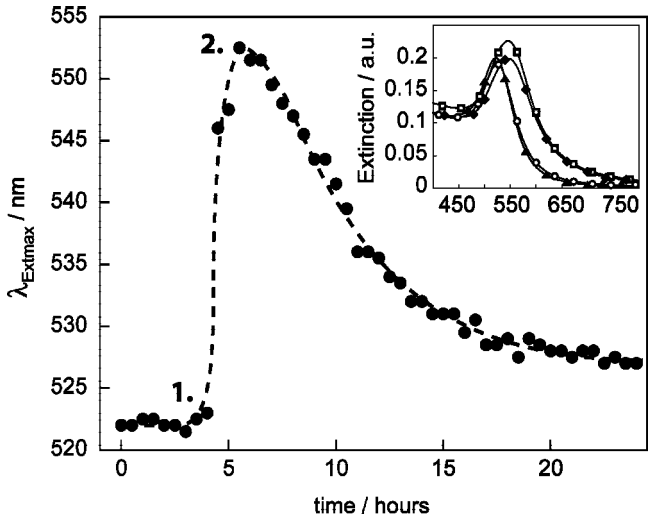

Figure 6. Addition of $JR2KC_2$ (**1**) caused a rapid folding induced bridging and aggregation that was reversed upon addition of 20 mM TCEP (**2**), which resulted in a blue-shift of the LSPR peak position (hatched line drawn as a guide for the eye). Inset: Extinction spectra of (▲) JR2EC functionalized particles ($t = 0$ h), (□) after addition of 2.5 μM $JR2KC_2$ ($t = 5$ h), (♦) after addition of 20 mM TCEP ($t = 6$ h), and (○) fully redispersed particles ($t = 72$ h).

Aggregation could be reversed by reducing the disulphide bridge that connects the two four-helix bundles. The polypeptides thus work as a highly selective "glue" for the spatially controlled assembly of gold nanoparticles, with properties suitable for use under physiological conditions. Polypeptide-folding as a means of inducing nanoparticle aggregation represents an interesting biomimetic route for nanofabrication, and the heteroassociating polypeptides constitute a new set of building blocks in the self-assembling hybrid/nanocomposite Lego reported previously by our group.[20,21]

Acknowledgment. During this study, D.A. was enrolled in the graduate school Forum Scientium and in the research programs Biomimetic Materials Science and NanoSense financed by the Swedish Foundation for Strategic Research (SSF). Financial support from CeNano and the Swedish Research Council (VR) is also gratefully acknowledged.

Supporting Information Available: Amino acid sequences, experimental details on polypeptide synthesis, nanoparticle synthesis, functionalization, and characterization. This material is available free of charge via the Internet at http://pubs.acs.org.

References

(1) Whitesides, G. M.; Grzybowski, B. *Science* **2002**, *295*, 2418–2421.
(2) Lehn, J.-M *Proc. Natl. Acad. Sci. U.S.A.* **2002**, *99*, 4763–4768.
(3) Shenhar, R.; Rotello, V. M. *Acc. Chem. Res.* **2003**, *36*, 549–561.
(4) Daniel, M. C.; Astruc, D. *Chem. Rev.* **2004**, *104*, 293–346.
(5) Niemeyer, C. M. *Angew. Chem., Int. Ed.* **2001**, *40*, 4128–4158.
(6) Mirkin, C. A.; Letsinger, R. L.; Mucic, R. C.; Storhoff, J. J. *Nature* **1996**, *382*, 607–609.
(7) Alivisatos, A. P.; Johnsson, K. P.; Peng, X.; Wilson, T. E.; Loweth, C. J.; Bruchez, M. P.; Schultz, P. G. *Nature* **1996**, *382*, 609–611.
(8) Verma, A.; Srivastava, S.; Rotello, V. M. *Chem. Mater.* **2005**, *17*, 6317–6322.
(9) Ryadnov, M. G.; Ceyhan, B.; Niemeyer, C. M.; Woolfson, D. N. *J. Am. Chem. Soc.* **2003**, *125*, 9388–9394.
(10) Stevens, M. M.; Flynn, N. T.; Wang, C.; Tirrell, D. A.; Langer, R. *Adv. Mater.* **2004**, *16*, 915–918.
(11) Lévy, R. *ChemBioChem* **2006**, *7*, 1141–1145.
(12) Reynolds, A. J.; Haines, A. H.; Russell, D. A. *Langmuir* **2006**, *22*, 1156–1163.
(13) Chen, Y.-J.; Chen, S.-H.; Chien, Y.-Y.; Chang, Y.-W.; Liao, H.-K.; Chang, C.-Y.; Jan, M.-D.; Wang, K.-T.; Lin, C.-C. *ChemBioChem* **2005**, *6*, 1169–1173.
(14) Elghanian, R.; Storhoff, J. J.; Mucic, R. C.; Letsinger, R. L.; Mirkin, C. A. *Science* **1997**, *277*, 1078–1081.
(15) Lee, J. S.; Han, M. S.; Mirkin, C. A. *Angew. Chem., Int. Ed.* **2007**, *46*, 4093–4096.
(16) Boal, A. K.; Ilhan, F.; DeRouchey, J. E.; Thurn-Albrecht, T.; Russell, T. P.; Rotello, V. M. *Nature* **2000**, *404*, 746–748.
(17) Chah, S.; Hammond, M. R.; Zare, R. N. *Chem. Biol.* **2005**, *12*, 323–328.
(18) Baltzer, L.; Nilsson, H.; Nilsson, J. *Chem. Rev.* **2001**, *101*, 3153–3163.
(19) Pandya, M. J.; Spooner, G. M.; Sunde, M.; Thorpe, J. R.; Rodger, A.; Woolfson, D. N. *Biochemistry* **2000**, *39*, 8728–8734.
(20) Aili, D.; Enander, K.; Rydberg, J.; Nesterenko, I.; Björefors, F.; Baltzer, L.; Liedberg, B. *J. Am. Chem. Soc.* **2008**, *130*, 5780–5788.
(21) Aili, D.; Enander, K.; Rydberg, J.; Lundström, I.; Baltzer, L.; Liedberg, B. *J. Am. Chem. Soc.* **2006**, *128*, 2194–2195.
(22) Enander, K.; Aili, D.; Baltzer, L.; Lundström, I.; Liedberg, B. *Langmuir* **2005**, *21*, 2480–2487.
(23) Nilsson, K. P. R.; Rydberg, J.; Baltzer, L.; Inganäs, O *Proc. Natl. Acad. Sci. U.S.A.* **2003**, *100*, 10170–10174.
(24) Olofsson, S.; Johansson, G.; Baltzer, L *J. Chem. Soc., Perkin Trans. 2* **1995**, 2047–2056.
(25) Olofsson, S.; Baltzer, L. *Fold. Des.* **1996**, *1*, 347–356.
(26) Ellman, G. L. *Arch. Biochem. Biophys.* **1959**, *82*, 70–77.
(27) Mie, G. *Ann. Phys.* **1908**, *25*, 377–445.
(28) Kelly, K. L.; Coronado, E.; Zhao, L. L.; Schatz, G. C. *J. Phys. Chem. B* **2003**, *107*, 668–677.
(29) Kreibig, U.; Vollmer, M. *Optical Properties of Metal Clusters*;Springer: New-York, 1995.

(30) Lazarides, A. A.; Schatz, G. C. *J. Phys. Chem. B* **2000**, *104*, 460–467.
(31) Storhoff, J. J.; Lazarides, A. A.; Mucic, R. C.; Mirkin, C. A.; Letsinger, R. L.; Schatz, G. C. *J. Am. Chem. Soc.* **2000**, *122*, 4640–4650.
(32) Storhoff, J. J.; Elghanian, R.; Mucic, R. C.; Mirkin, C. A.; Letsinger, R. L. *J. Am. Chem. Soc.* **1998**, *120*, 1959–1964.
(33) Aili, D.; Tai, F.-I.; Enander, K.; Baltzer, L.; Liedberg, B. *Angew. Chem., Int. Ed.* In press.
(34) Weeraman, C.; Yatawara, A. K.; Bordenyuk, A. N.; Benderskii, A. V. *J. Am. Chem. Soc.* **2006**, *128*, 14244–14245.

NL8014796